

BINDURA UNIVEESITY OF SCIENCE EDUCATION

FACULTY OF SCIENCE AND ENGINEERING

DEPARTMENT OF CHEMISTRY



**Absorptive removal of crystal violet dye from wastewater effluent from textile industry
using biochar synthesized from corn stalks**

TINASHE SIMBINE (B1953907)

Supervisor: Mr. Katengeza

**A DISSERTATION SUBMITTED IN PARTIAL FULFILMENT OF THE
REQUIREMENTS OF THE BACHELOR OF SCIENCE HONOURS DEGREE IN
CHEMICAL TECHNOLOGY(HBScCHT)**

(June 2023)


APPROVAL FORM

The undersigned certify that they have supervised, read and recommend to the Bindura University of Science Education for the acceptance of a research dissertation entitled:

Absorptive removal of crystal violet dye from wastewater effluent from textile industry using biochar synthesized from corn stalks

Submitted by Tinashe Simbine

In the partial fulfilment of the requirements for the Bachelor of Science Education Honors Degree in Chemical Technology.


.....

(Signature of student)

...26/05/2023...

Date


.....

(Signature of Supervisor)

18/09/2023
.....

Date

DECLARATION FORM

I, Tinashe Simbine do hereby declare to the best of my knowledge to Bindura University of Science Education that this dissertation is my original work and all materials and academic sources of information other have been duly acknowledged. I also declare that this current work has not been submitted to any other academic institution for the purposes of an academic merit.

Signed..... Date26/05/2023.....

DEDICATION

I dedicate this work to my family, especially my mother who have been there to support me in every move of my study. I also want to appreciate my friends and colleagues for an undivided support through this academic work.

ACKNOWLEDGEMENTS

My sincere gratitude goes to my project supervisor Mr. Katengeza and the Bindura University of Science Education chemistry laboratory technicians and staff for their support and academic guidance on my experiments done in this study. I also acknowledge the university lab personnels for providing chemical reagents and apparatus required for this study to be a success.

List of tables

Table 2.1 Agricultural biomass wastes that can be used to adsorb dyes from water ..	6
Table 4.2 The best fit experimental parameters to describe the adsorption.....	23
Table 4.3 Thermodynamics parameters for the adsorption process	24

List of Figures

Figure 2.1	Chemical structures of some basic dyes (Chakraborty et al.,2011)	4
Figure 3.2	The process flow diagram for biochar synthesis	10
Figure 4.3	pHpzc plot for CS biochar	17
Figure 4.4	The effect of CS biochar dosage	18
Figure 4.5	The effect of contact time	19
Figure 4.6	The effect of temperature	20
Figure 4.7	The Langmuir adsorption isotherm modelling	21
Figure 4.8	The Freundlich adsorption isotherm modelling	21
Figure 4.9	Pseudo first order kinetic model for the adsorption	22
Figure 4.10	Pseudo second order kinetic model for the adsorption of CV	23
Figure 4.11	Thermodynamics plot of the adsorption process	25

Table of Contents

APPROVAL FORM	ii
DECLARATION FORM	iii
DEDICATION	iv
ACKNOWLEDGEMENTS	v
List of tables	vi
List of Figures	vii
Key words	x
Abbreviations	xi
Abstract	xii
Chapter One	1
1.0 INTRODUCTION	1
1.1 Problem statement	2
1.2 Justification	3
1.2 Objectives and Aims	3
Chapter Two	4
2.0 Literature Review	4
2.1 Biochar surface functional groups	7
2.2 Environment and the usage of biochar	7
Chapter Three	9
3.0 Materials and methodology	9
3.1 Materials	9
3.2 Biochar synthesis	9
3.3.0 Characterization of biochar	11
3.3.1 Sampling of wastewater	11
3.3.2 Sample preparation	11
3.3.3 Preparation of standards	12
3.3.4 Batch absorption experiments	12
3.4.0 Data treatment	13
3.4.1 Adsorption capacity	13
3.4.2 Percentage removal	13
3.4.3 Adsorption isotherm modeling	14

3.4.4 Freundlich isotherm	14
3.5 Thermodynamic Study	15
Chapter Four	16
4.0 Results and Discussion	16
4.1.0 The absorbent surface analysis	16
4.2.0 Adsorption study	17
4.3 Adsorption isotherm modeling	20
4.4 Adsorption kinetics	22
4.5 Adsorption thermodynamics model	24
4.6 Comparisons of the findings of this work with the relevant literature	26
Chapter Five	27
5.0 Conclusion and Recommendation	27
6. References	28
Appendix.....	33
i. Raw data and spectroscopic data	33
The calibration curve for cryastal violet dyes obtained	35
Raw data	36

Key words

1. Crystal violet
2. Corn stalks
3. Biochar
4. Adsorption
5. Pollutants
6. Waste water
7. Kinetics
8. Isotherms
9. Thermodynamics
10. Dyes
11. Equilibrium

Abbreviations

CS – corn stalks

CV – crystal violet

MB – methylene blue

Zpc – zero-point charge

AC – activated carbon

ZVI – zero valent iron

DW – deionized water

UV-vis – ultraviolet visible spectroscopy

FT-IR – Fourier transform Infrared spectroscopy

%R – percentage removal

Abstract

The toxic (crystal violet) dyes are rapidly increasing in their concentrations in the environment and water ways, due to increase in their application in textile industry. The dyes enter the food chain and water system through the releasing of untreated textile industry water effluent into the environment. They contaminate underground water through leaching in the soil and some are washed away into the rivers and streams thereby causing water pollution and destroying the aquatic ecosystem. Exposure or consume of dye-containing foods is harmful to all living organisms, they are also carcinogenic substances. Therefore, elimination of these dyes from water is very important to save lives and the ecosystem. The adsorption method was used in this study since it is eco-friendly and simple and straightforward to use. The adsorbent was synthesized through pyrolysis of biomass based, corn stalks in a low oxygen environment at 400°C. The produced corn stalks biochar was characterized for point zero charge (pH_{pzc}) and the functional groups present were analyzed using the FT-IR instrument. The effect of biochar dosage on the adsorption rate was examined at (0.5g, 1.0g, 1.5g and 2.0g) and the maximum percentage removal was achieved at 2.0g at room temperature. The effect of temperature, contact time and pH on the adsorption process were also investigated, with the highest percentage removal(%R) achieved at 25°C for 70.97%, 68.05% after 30mins and 62% at pH = 8 respectively. The Langmuir adsorption isotherm model explained better the nature of the adsorption of the crystal violet onto CS biochar ($R^2 = 0.6924$) which is a monolayer adsorption. The pseudo first order kinetics was used to explain the kinetic nature of the experimental data due to its larger correlation coefficient ($R^2 = 0.9547$). The adsorption was feasible and spontaneous since the Gibbs free energy was negative and $\Delta H = -0.821 \text{ kJ/mol}$ was also negative at room temperature indicating that the process was exothermic.

Chapter One

1.0 INTRODUCTION

The quality of water supplies is deteriorating day by day as a result of numerous anthropogenic activities, uncontrolled urbanization, and growing industrialization. One of the main causes of water pollution is the release of harmful dyes such as crystal violet in wastewater produced by textile dyeing companies (Bilal et al. 2016). A few examples of industrial sources that discharge these organic substances known as dyes include the paper printing, leather, rubber, cosmetic, and textile industries (Piaskowski et al., 2018; Katheresan et al., 2018). The number of dyes delivered annually to satisfy modern demand is estimated to be between 0.7 and 1.6 million tons, and 10-15% of this volume is disposed of as wastewater, making it one of the primary causes of water pollution (Bhatia et al., 2017; Varghese et al., 2019; Syafiuddin and Fulazzaky, 2020).

At any point of the textile production process (in the creation of fiber, yarn, fabric, or on finished textiles), fabric can be colored (Bullon et al, 2017). When the waste-water from these processes is discharged into the environment, the crystal violet dye contaminants leach into the underground contaminating drinking water and some accumulating in the soil and some are disposed in the drainages thereby finding their ways into the rivers and other water bodies (Akhta et al., 2021).

These dyes are highly persistent and non-biodegradable, and their buildup always leads to poor oxygenation of the aqueous environment by impeding the photosynthesis of photosynthetic organisms (Misra et al., 2020; Xu et al., 2018). As a result, they pose a serious threat to the environment's ecology. In addition, most dyes are toxic, mutagenic, and carcinogenic, endangering aquatic life as well as human health (Ramamoorthy et al., 2020). Excessive dye exposure can also cause respiratory problems, skin irritation, and cancer. Therefore, it is crucial to remove colors from wastewater in order to ensure the safe release of treated effluent into streams (Amirza et al. 2017).

Reverse osmosis, ion exchange, electrodialysis, electrolysis, and adsorption techniques are some of the treatment methods that are frequently used to treat dye-contaminated water (Guo et al., 2019; Ahmad et al., 2015). Various technologies have been developed to treat water that contains dyes, including biological processes, membrane processes, chemical and electrochemical technology, and membrane technology. Some of the disadvantages of most of these technologies include the production of hazardous sludge, high operating and maintenance costs, and the difficult treatment procedure (Yahiaoui et al. 2021). The removal of crystal violet from wastewater using activated carbon as the adsorbent has been demonstrated in various treatment of water effluents containing dyes (Hegazi et al., 2013). However, this method is costly since it involved the use of activated carbon. This encourages the development of less expensive, greener materials for degrading organic pollutants (dyes) from contaminated water.

Using biochar made from corn stalks is a practical and affordable way to eliminate toxic dyes from wastewater due to its porous surface absorptive ability.(Dai et al., 2019). A carbonized solid by-product of biomass produced by pyrolysis under high temperature and low oxygen conditions is called biochar. (Seow et al. 2022).

1.1 Problem statement

The application of dyes in textile industries has increased tremendously due to growth in textile manufacturing companies across the globe. The crystal violet is the commercial type of dye which is commonly applied for purposes such as textile dyeing and give fabrics or wools desired colors. The water effluent from these textile industries constitutes significant concentrations of the crystal violet dyes and other toxic chemicals. The waste-water discharge from these dyeing industries poses environmental pollution and cause serious damage to living organisms including aquatic life. The elimination of crystal violet from water through adsorption before discharge into the environment mitigate serious health issues and potential environmental hazards. The corn stalks bio-sorbent was chosen in this study because of its easy to prepare and cost effective in treated dye-contaminated water.

1.2 Justification

Cationic dyes , such as crystal violet CV are becoming more and more polluting in water sources and in drinking water due to their variety application in industry such as for dyeing papers, textile fibers, plastics, leathers and pharmaceuticals. The elimination of these dye contaminants is crucial since they contribute to a range of health hazards includes cancer, neurotoxins and affects soil fertility ,by entering the water system . For that reason, biochar has become more popular because of its straightforward and inexpensive synthesis, The corn stalks are biomass materials which can be easily obtained from the farms after maize harvesting.

1.2 Objectives and Aims

The aims of this study are to accurately remove poisonous crystal violet dyes from wastewater effluent from textile industry using eco-friendly and low-cost approach.

The objectives of the study are:

1. to synthesize biochar through pyrolysis of corn stalk in a low oxygen environment
2. to characterize biochar
3. to remove crystal violet dyes from waste-water

Chapter Two

2.0 Literature Review

In order to give fabrics a specific color, dyes are applied to the cloth. In the textile industry, a variety of fabric dyes are employed (Samanta et al., 2011). Natural and artificial colors are the two main categories. Extraction of natural pigments from plants, animals, and minerals is the process used to create natural colors. In a laboratory, man-made synthetic cloth dyes are created (Affat, 2021). Any stage of the textile production process—in the creation of fiber, yarn, fabric, or on the surface of completed textiles—can involve dyeing cloth (Bullon et al., 2017).

Basic dyes are cationic pigments that are frequently used to color fabrics like wool, nylon, natural silk, and various altered acrylic fabrics (Mani ; Bharagava 2018). This is a common preference in the fabric industry and is certainly one of many different types of textile dyes (Carr , 2012). Usually, acetic acid is added to the dye bath to increase the color's absorption. This dye is also frequently used to alter the color of paper (Bhuiyan et al., 2013).

Methylene blue (MB) and crystal violet (CV) are examples of low-cost cationic dyes and widely useful in textile and paper industry. Their structures are shown below in **Fig 2.1**

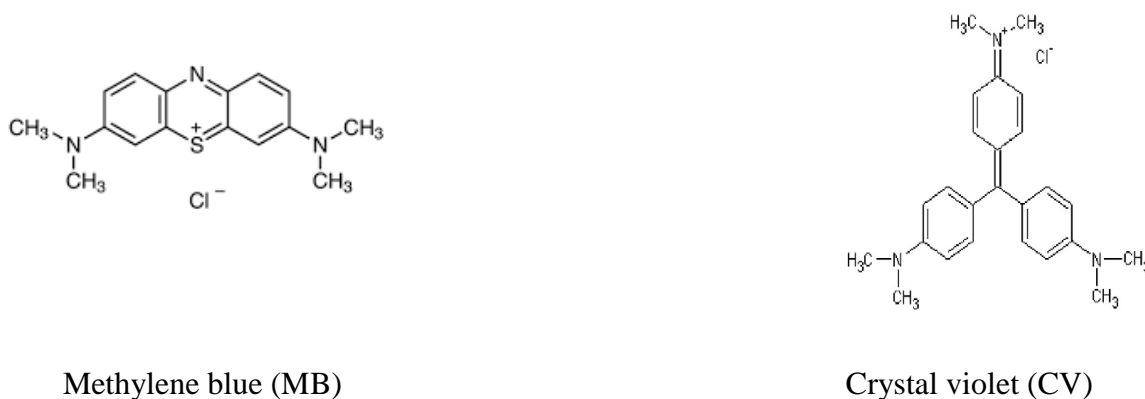


Figure 2.1 Chemical structures of some basic dyes (Chakraborty et al.,2011)

Synthetic dyes are extremely toxic substances that have a detrimental impact on all life forms because they contain substances like sulfur, naphthol, vat dyes, nitrates, and acetic acid (Kant, 2011). However, environmentalists are growing increasingly concerned about their use in the textile industry. The estimated 700,000 tons of dyes produced annually around the world are discharged as industrial waste in about 20% of those cases without being treated (Ghorai, 2014; El-Maghraby et al., 2011).

These dyes pose a serious risk to both human health and water quality as a result, making them a pressing issue. The effects of dye exposure on the organisms exposed can be acute or chronic, depending on the exposure time and dye concentration (Alderete et al., 2021). Skin rashes, cancer, mutations, and other health problems can occur as a result of dye exposure. Discharging wastewater containing dyes into natural streams and rivers seriously harms aquatic life, the food chain, and the aesthetic qualities of the environment (Al-Tohamy et al., 2022). The dyes present in our water bodies can also prevent aquatic plants from producing photosynthesis, as dyes like CV have a tendency to absorb and reflect sunlight into water (Ahmad et al., 2006).

In order to stop the discharge and pollution of wastewater, numerous wastewater treatment techniques have been continuously used to remove these dyes (Chen et al., 2017; Saber-Samandari et al., 2017). When assessing economics, applicability, and removal efficacy, adsorption is recommended as the preferred technique (Rasalingam et al., 2015). The most important variable affecting removal effectiveness is the selection of adsorbents (Zhang et al., 2020). Activated carbon (AC) is the most effective adsorbent, but its high cost limits its use. A variety of bio-based biochar has been produced from agricultural wastes, such as fruit peel, crop straw, coconut shell, and vegetable residues, according to recent studies and experiments conducted to assess the applicability, effectiveness, and affordability of the adsorption method (Mishra et al., 2021). The zero valent iron (ZVI) and porous adsorbents with large surface areas and reaction sites have also been combined to create iron-based porous materials that are effective adsorbents for removing toxic dyes from wastewater (Wang et al., 2012).

In the similar studies conducted, it was demonstrated that iron-modified montmorillonite could effectively adsorb crystal violet (CV) (Guz et al., 2014) and that iron nanoparticles painted onto three-dimensional graphene could efficiently and quickly degrade azo dye (Wang et al., 2013). ZVI's use in actual water treatment is limited because it tends to aggregate and is quickly

oxidized (Zhou et al., 2018). In order to find different matrices that will stop iron particle aggregation, numerous studies have been launched. For instance, iron has been added to montmorillonite to aid toxic cationic dyes in binding onto to it (Liu et al., 2018), and iron nanoparticles have been added to three-dimensional graphene to aid azo dyes in degrading (Liu et al., 2018).

A variety of agricultural and forestry waste materials' biosorption capacities and the reagents required to activate them are listed in **Table 2.1**. The bio-sorbents have been activated using various acids to increase their porosity, specific surface area, binding sites, and aqueous solution chemistry. Phosphoric acid, for example, induces bond cleavage in agricultural waste biomass to increase the carbon yield (Bello et al., 2019). The biosorption of color was facilitated by phosphoric acid, and the summary of adsorption studies is shown below (**Table 2.1**).

Table 2.1 Agricultural biomass wastes that can be used to adsorb dyes from water.

Source of biowaste	Modified with	Type of dye used	Dye concentration (mg/L)	Optimum pH	Removal efficiency (%)	Adsorption capacity (mg/g)	Optimal sorbent dose(g/L)	References
Grass waste	Phosphoric acid	MB	20	7		241.2	0.8	Jawad et al,2020
Dead leaves of oak trees	No modification	CV	50	7	80	31.65	0.1	Sulyman and Gierak, 2020
corncoobs	KOH and heat	MB	150	5	99.53	523.18	0.3	Sun et al., 2021
Activated carbon	HCl solution	Allura Red AC	60	2	90	287.1	0.5	Streit et al., 2019
Sea plant	-	MB	50	7	57	27.78	0.1	Astuti et al., 2019

Studies have shown that, waste products from agriculture and forestry are often high in cellulose, hemicellulose, and lignin (Li et al., 2016). The active groups present on their surfaces include hydroxyl, carboxyl, amino, carboxyl, methyl, and others (Zhou et al., 2019). These active groups can adsorb dyes by mechanisms such as complexation, hydrogen bonding, ion exchange, and more (Dai et al. 2018). The most important characteristics of a good adsorbent are typically regarded as surface area, empty active sites, and repeatability in the activation processes (Leng et al., 2021). The biomass-derived adsorbent is preferred in comparison because it has the highest surface area, which increased the adsorption of pollutants depending on the source types, regardless of the activation methods used. However little information has been gathered for far on how well corn stalks biochar can remove crystal violet from water.

2.1 Biochar surface functional groups

Important functional groups on the surface of biochar, which increase its capacity for sorption, include carboxylic (COOH), hydroxyl (OH), amine, amide, and lactonic groups.). Temperature and biomass are the two main factors that affect the surface functional groups of biochar. The number of functional groups in biochar may also diminish as other characteristics like pH, surface area, and porosity rise (Chen et al., 2014). The surface functional groups are identified using Fourier Transform Infrared Spectroscopy instrument.

The advantages of biosorption are influenced by the properties of the adsorbent material used in dye adsorption processes. The availability of a wide range of adsorbent materials, the ease of preparation or processing, and the requirements for activation are critically important for economy in addition to the concepts of green chemistry (Bulgariu et al., 2019).

2.2 Environment and the usage of biochar

Biochar has a wide range of applications, but in order to avoid unfavorable effects, it must be carefully considered how it will affect the environment. Prior to application, stability is the main factor that must be addressed. Biochar makes up the carbon structure. The stability of the carbon structure consequently affects the stability of biochar (Haung et al., 2019). The two primary indicators of the carbon structures in biochar are aromaticity and aromatic condensation (McBeath et al., 2014). The biochar's released dissolved organic material retains a high level of aromaticity, resilience, and stability.

As a result of the carbon that the biochar releases into the environment, water's carbon content increases when it is used to clean wastewater (Gupta et al., 2022). The creation of biochar from sludge that contains heavy metals may result in heavy metal contamination during the treatment process (Vikrant, 2018). After prolonged use, stability gradually deteriorates, just like when biochar serves as a catalyst. Structure-related problems might also be the root of the instability of biochar. As a result, stability of biochar is essential for environmental concerns. The toxicity of biochar to soil bacteria must be investigated prior to use (Premarathna et al. 2019),

In this current study, maize stalk was used as an accessible and practical adsorbent to test how well crystal violet dyes could be removed from aqueous solutions. The optimal removal efficiency was studied, along with the effects of contact time, pH, and adsorbent dose on the adsorption capacity.

The experimental data were evaluated using the pseudo-first order and pseudo-second order kinetic models.

Chapter Three

3.0 Materials and methodology

3.1 Materials

The corn stalks were obtained from a local maize field in Bindura and the wastewater effluent were collected from a local textile industry. The chemical reagents which include sodium hydroxide, hydrochloric acid, and crystal violet and apparatus were obtained from Bindura University of Science Education. All reagents used in this work were highly pure and of analytic grade, distilled water was used in all dilutions done in this study.

3.2 Biochar synthesis

The corn stalks (straws) were washed using deionized water and later dried at 80 °C in an oven for about 24 hours to remove moisture. The corn stalk small straws were pyrolyzed for 2 hours in Elsa stove at 400 °C in a low oxygen environment to produce biochar (BC). The biochar was then collected and allowed to cool at room temperature. The bio-sorbent (BC) were analyzed for functional groups present on its surface using the FT-IR instrument. The process flow diagram for the production of biochar through pyrolysis is shown below (**Fig 3.2**)

Flow diagram

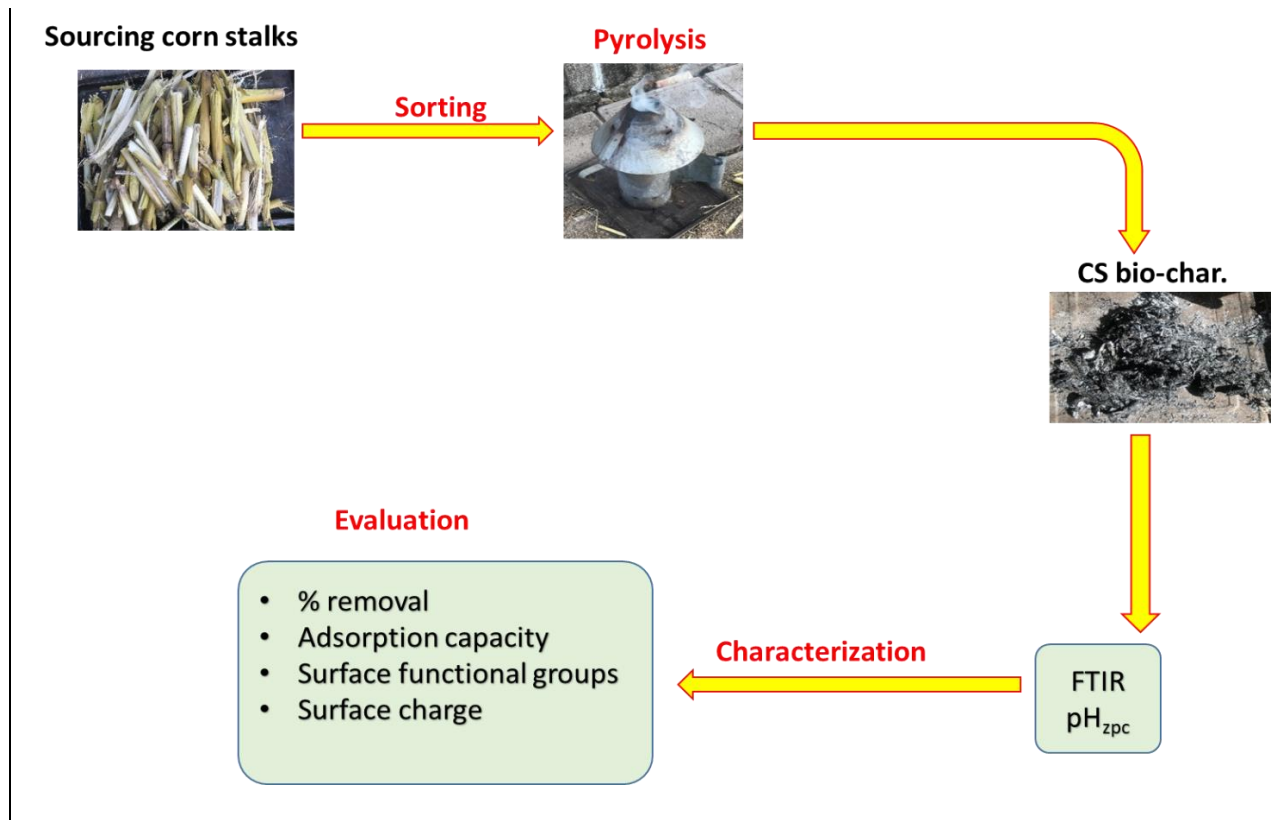


Figure 3.2 The process flow diagram for biochar synthesis

3.3.0 Characterization of biochar

About 0.5g of biochar were added to 25ml of deionized water (DW) and the pH and electrical conductivity were measured using pH meter and conductivity meter respectively. The surface character of the bio-adsorbent and the functional groups present were analyzed using the FT-IR spectroscopy (Nejadshafiee et al., 2019).

In order to determine pHPzc, the pH drift method was used (Lima et al., 2018). Both 0.01 M HCL and 0.01 M NaOH were used to prepare a 0.01 M solution of NaCl and get it to pH 2. In a conical flask, a 0.01 M solution of NaCl that had already been pH-adjusted to 2 was combined with a 1 g sample of biochar (BC). The combination was swirled, and it was left standing for 24 hours.

This investigation was done again at pH 4, 6 and 8. The sample mixture was filtered and the final pH was determined after 24 hours by utilizing a pH meter. The graph of the initial pH versus the pH change was obtained. The point zero charge (pHPzc) was determined on the graph (Al-Maliky et al 2021).

3.3.1 Sampling of wastewater

Wastewater samples were collected from a local textile industry water effluent in Bindura. The sample water was fetched using a 500 ml plastic jar with extended wire handle. The wastewater was taken from the top, middle and bottom of the reservoir, prior fetching, the water was stirred using a long wooden stick so that the water is evenly homogenized. The three samples collected were thoroughly mixed taken to the lab for treatment and analysis.

3.3.2 Sample preparation

The wastewater sample were filtered to remove suspended solids. the sample were transferred into 500 ml beaker and stirred to maintain its homogeneity. About 50 ml of the samples were measured and transferred into a 250 ml volumetric flask and filled to mark with distilled water

(DW). The concentration of dyes in the sample were analyzed before and after treatment with different BC dosage (0.50 g, 1.00 g, 1.50 g and 2.00 g) using UV-vis instrument.

3.3.3 Preparation of standards

The stock solution was prepared by accurately weigh 0.25 g of crystal violet into a 250 ml beaker followed by addition of DW then transferred into a 250ml volumetric flask and filled to mark with DW. The flask was closed with the stopper then shaken for 4minutes to dissolve the CV dye. The stock solution was diluted into other standards, 60 ppm, 40 ppm and 20 ppm. The calibration curve was obtained by running these standards in the UV-vis instrument at wavelength max 500 nm.

3.3.4 Batch absorption experiments

Bath experiments were conducted to study the effect of dosage, effect of temperature and effect of pH on the adsorption of the dyes on the surface of adsorbent. Time of conduct were also verified by analyzing the concentration of the contaminants at 10 minutes intervals for 40minutes using optimum BC dosage (1.00 g) at room temperature and pH 6.5. To check the effect of pH, batch experiments were conducted at pH 4, 6 and 8. The pH were adjusted using 0.1 M HCl and 0.1M NaOH solutions (Munagapati ,.2016). The effect of temperature was observed when the adsorption processes carried out at optimum BC dosage at temperatures; 25 °C 30 °C, 40 °C, 50 °C and 60 °C at pH of 6.5.

A measuring cylinder were used to measure four sets of 75mL of the sample and transferred into 250ml beakers. Different biochar dosage (0.50 g, 1.00 g, 1.50 g and 2.00 g) was added into four samples respectively. The mixture was agitated at 200rpm and controlled temperature shaker for 20mins then filtered. The final crystal violet concentrations in the filtrate were analyzed using the UV/vis instrument

3.4.0 Data treatment

3.4.1 Adsorption capacity

The BC adsorption capacity were determined using the following equation

$$q_t = \frac{C_o - C_t}{m} * V \quad (1)$$

Where C_o and C_t are the initial and final pollutants concentrations (mg/L) at time, t, m is the mass of adsorbent dosage (g) and V is the volume(ml) of sample used.

3.4.2 Percentage removal

The waste water pollutants were analyzed before and after treatment using the UV-vis instrument. The percentage removal, %R were calculated as follows

$$\text{Dye \%R} = \frac{C_o - C_t}{C_o} * 100 \quad (2)$$

Where C_o and C_t are the initial and final pollutants concentrations (mg/L) at time, t respectively

The adsorption capacity at equilibrium q_e (mg/g) is given by the following equation

$$q_e = \frac{C_o - C_e}{m} * V \quad (3)$$

Where C_o and C_e are the initial and final pollutants concentrations (mg/L) at equilibrium, e respectively. The adsorbent mass, m (g) and volume, V of the contaminated water (ml)

3.4.3 Adsorption isotherm modeling

The Langmuir isotherm model explains monolayer adsorption onto a surface of identical sites and the adsorption onto a certain surface has no effect on the neighboring sites

$$\frac{C_e}{q_e} = \frac{1}{Q_o K} + \frac{C_e}{Q_o} \quad (4)$$

Where q_e is the total amount of dyes adsorbed (mg/g) or equilibrium adsorption capacity

The adsorption parameters were obtained by the plotting of the graph of C_e/q_e versus C_e in the Langmuir equation (4), Q_o and K are Langmuir constants. (Muhammad., et al 2019)

The nature of the isotherm was also studied using the Langmuir model shown in equation (5) below

$$q_l = \frac{1}{1+KC_o} \quad (5)$$

Where q_l is the separation factor or equilibrium parameter, K is the Langmuir constant and C_o is the initial dye concentration in mg/L (Muhammad., et al 2019)

3.4.4 Freundlich isotherm

The Freundlich isotherm model helps to explain the homogeneity of the adsorbent surface and the surface energies.

$$\ln Q_e = \ln K + \frac{1}{n} \ln C_e \quad (6)$$

Where, K and n are Freundlich constants(L/mg) , Q_e is the adsorption capacity(mg/g) and C_e is the dye concentration at equilibrium (Macedo et al., 2006)

3.5 Thermodynamic Study

The effects of temperature on the adsorption process were analyzed and the thermodynamic parameters including ΔH , ΔS , and ΔG were also calculated based on the adsorption isotherms. The specific calculation method is shown as in equations (7) and (8), respectively. (Zhang et al., 2020).

$$\Delta G = -RT \ln \frac{Q_e}{C_e} \quad (7)$$

$$\ln \frac{Q_e}{C_e} = \frac{\Delta S}{R} - \frac{\Delta H}{RT} \quad (8)$$

Where ΔG is the Gibbs free energy (Kj/mol) , ΔS is entropy change(Kj/mol/ °C), ΔH is the enthalpy change of reaction (Kj/mol). R is the constant (8.314 J/mol.K) and T is the absolute temperature (Chaukura et al., 2016).

Chapter Four

4.0 Results and Discussion

4.1.0 The adsorbent surface analysis

The FT-IR and electrical conductivity results of the adsorbent surface functional groups await. The corn stalks biochar synthesized had a pH of 7.9 which suggest that it formed alkaline solutions when added to distilled water'

4.1.1 The pH_{pzc} and the effect of pH

The pH_{pzc} of corn stalk biochar was 7.3 (**Fig 4.3**) showing that the surface of the adsorbent will be positively charged at pH lower than 7.3 and negatively charged at pH greater than pH_{pzc} value (Yahya et al., 2008). From a pH range of 4.0 to 8.0, the impact of pH on the adsorption of CV was examined. Higher pH levels were seen to result in an increase in the percentage elimination efficiency. It was noted that the percentage elimination crystal violet from water increased from 46% to 62% at pH 4 to 8.0 respectively. The rivalry that develops for the active site on the adsorbents between the excess concentration of H^+ ion and the cationic component of the dye may be the cause of the reduced removal of the dye at lower acidic pH values.

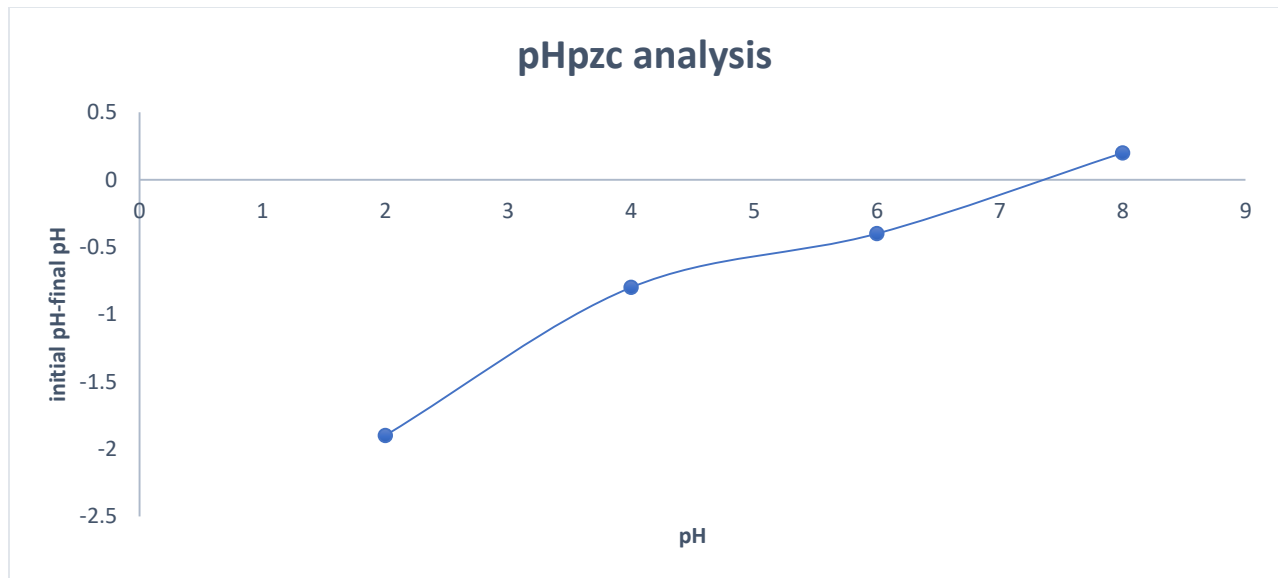


Figure 4.2 pHpzc plot for CS biochar

The removal of the dyes at higher pH values will be electrostatic interaction since the surface will be charged oppositely to the dyes which are cationic in nature.

4.2.0 Adsorption study

4.2 .1 Dosage effect

The adsorbent dosage effect study , for the adsorption of the dye onto CS biochar was verified as show in the (**Fig 4.4**). The residual concentration of CV decreased exponentially, as the amount of the CS biochar dose increases from 0.5g to 2.0 g. This trend was due to increase in more active sites on the surface of the adsorbent (Lin et al.,2011). Dosage at 0.5 g has the least removal of the dyes (has the highest residual concentration of dyes) because the porous active sites were all occupied and there were fewer to allocate more contaminants molecules. The active sites quickly saturate. The maximum adsorption was attained at 2.0 g because there was more active sites to interact with the contaminants (**Fig 4.4**)

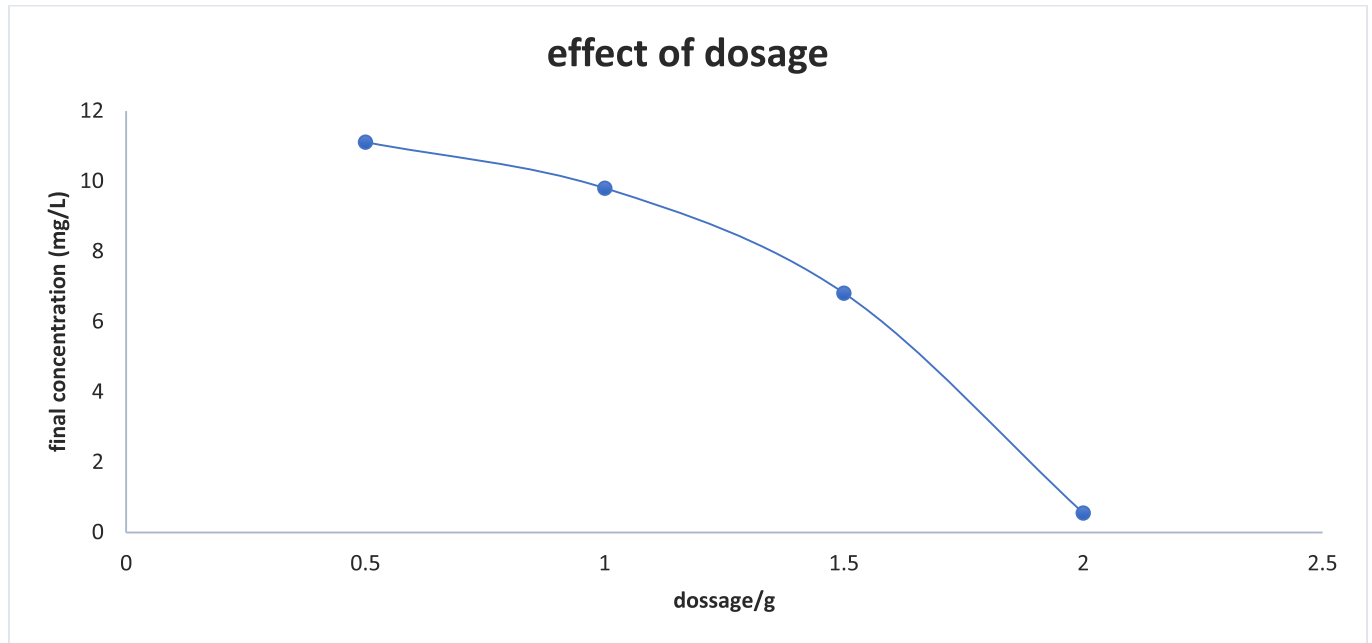


Figure 3.4 The effect of CS biochar dosage

The initial CV concentration before treatment was 19.11 mg/L and this decreased to 11.63 mg/L after shaking the dye-contaminated water with 0.5 g of CS bio-sorbent. The concentration of the CV dyes further dropped to 1.30 mg/L after 2.0 g of the biochar added. This proves that the dye removal efficiency of the bio-sorbent used in this experiment increases with amount added.

4.2.2 Effect of conduct time

Results from an investigation on the impact of Crystal Violet's adsorption contact time with corn stalks are displayed in (Fig 4.5). The figure shows that a quick adsorption that gets stronger over time explains the percentage removal (%R) rate of CV onto CS cornstalk. The percentage removal of CV after first 10mins was 14.43% this showed that the pollutants and the adsorbent were not yet interacted enough in the solution. The section in Fig 4.5 where there are no discernible change shows that the equilibrium time for the dye's adsorption was attained at 68.05% for 30 minutes. After 30 minutes there was no noticeable change in the percentage removal because all active sites were dye-saturated. The maximum percentage removal (68%) of the pollutants was achieved in 30mins of the process.

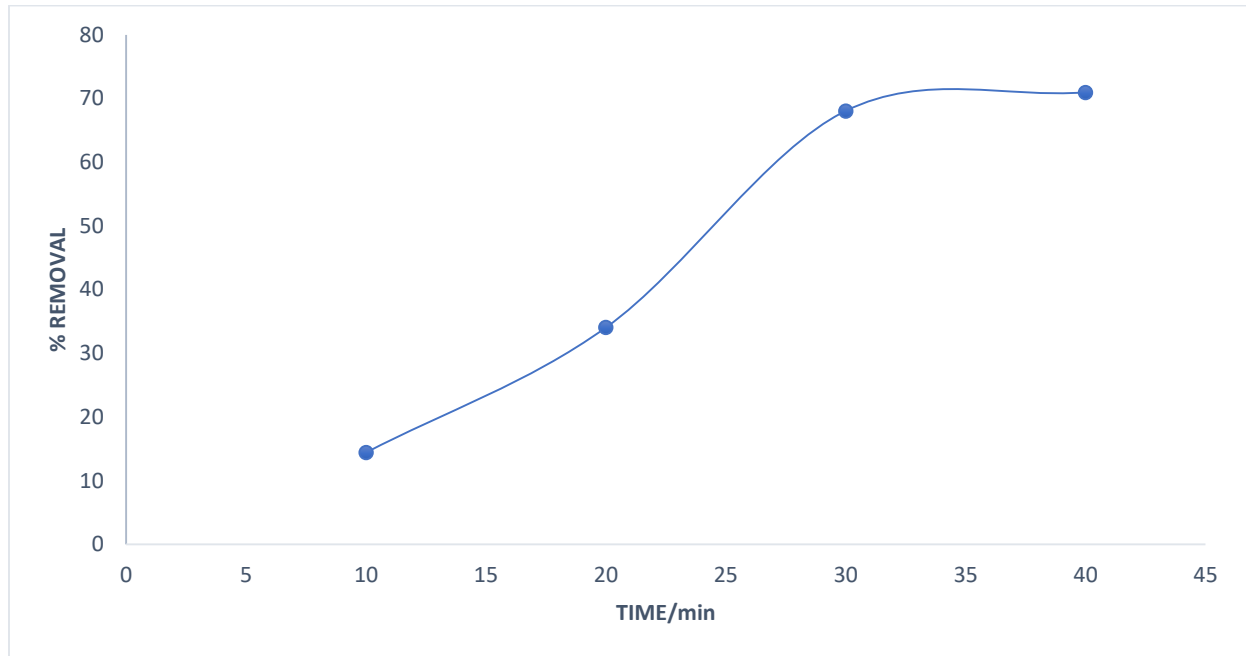


Figure 4.4 The effect of contact time

4.2.3 Effect of temperature

Figure 4.6, shows the variations in CV's adsorption capacity at various temperatures. It was discovered that the adsorption capacity of CV decreases as the temperature increase from 25°C to 60°C, meaning that the adsorption of dye molecules might be an exothermic and spontaneous process. The increase in temperature slows down the adsorption process. This demonstrates that the binding forces between the adsorbent and the adsorbate diminish as the temperature rises. These findings are in line with those made by Jabar et al. (2022) with regards to the adsorption of crystal violet dye using biochar made from cocoa leaves. The maximum adsorption capacity was achieved at 25°C of 70.97% and dropped to 12.06% as temperature increased to 60°C in **(Fig 4.6)**.

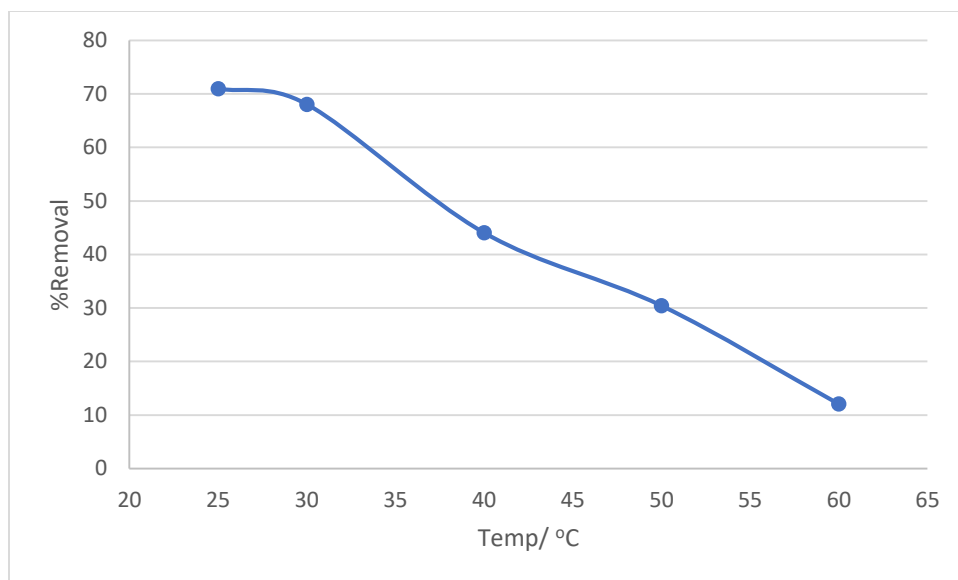


Figure 4.5 The effect of temperature

4.3 Adsorption isotherm modeling

In order to quantitatively compare the behavior of adsorbents under various experimental conditions, the adsorption isotherm is crucial for describing how the adsorbate interacts with the adsorbent and for reliably predicting the adsorption parameters.

Two widely used models, the Freundlich model and the Langmuir model, were selected to simulate the adsorption isotherms in this study and to explain the interaction between the CS biochar and the organic dye pollutant.

The Langmuir adsorption explains well the experimental data obtain from this study. The correction coefficient ($R^2 = 0.6924$) in (**Fig 4.7**) which is higher than obtained from Freundlich adsorption isotherm model ($R^2 = 0.0057$) in **Fig 4.8**. This suggest that the adsorption of crystal violet onto corn stalk biochar sites was a monolayer adsorption and there was no transmigration of dye molecules adsorbed onto a particular site of the adsorbent. The Langmuir constant (K) obtained from the experimental data shows that the adsorbent reached its maximum adsorption capacity at 8.60 mg/g when ($K = 1.53$). The Langmuir equilibrium separation factor, $ql = 0.026$ (equation 5) which shows that the adsorption of CV to the adsorbent was favorable since $ql < 0$

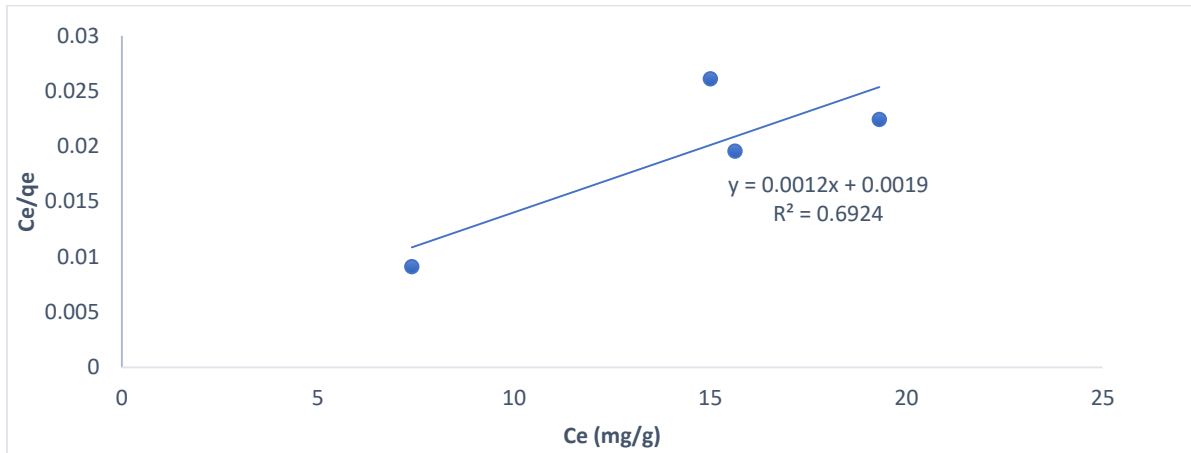


Figure 4.6 The Langmuir adsorption isotherm modelling

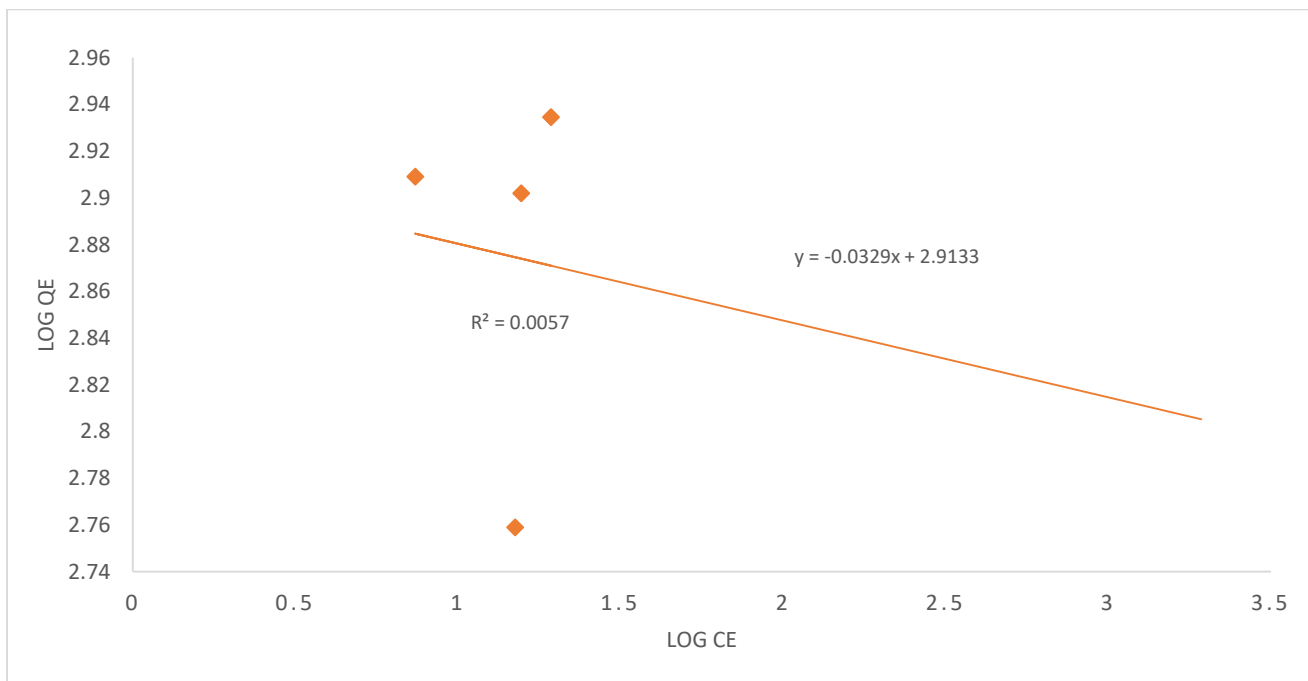


Figure 4.7 The Freundlich adsorption isotherm modelling

4.4 Adsorption kinetics

The pseudo-first order kinetic model explains the adsorption mechanism across the entire contact time range. **Table 4.2** demonstrates that the R^2 values obtained in experimental data for pseudo first order kinetics is higher than R^2 for the pseudo second order kinetic model. Due to a high correlation coefficient determination, R^2 value for pseudo 1st order plot (**Fig 4.9**) the adsorption was best fit the pseudo-first order kinetic model. The pseudo first order and second order were $R^2=0.9547$ (**Fig 4.9**) and $R^2 = 0.7669$ (**Fig 4.10**) respectively. This explains that rate determining step of adsorption of CV onto adsorbent maybe physisorption, the adsorbate formed physical bonds with surface of the adsorbent. The dyes molecules only occupied the porous sites of the corn stalk biochar and did not form chemical bonds on the sites. The chemisorption was expected when the experiments were carried out in an alkaline medium because the CS sites will be negatively charged and attract the cationic species (dyes)

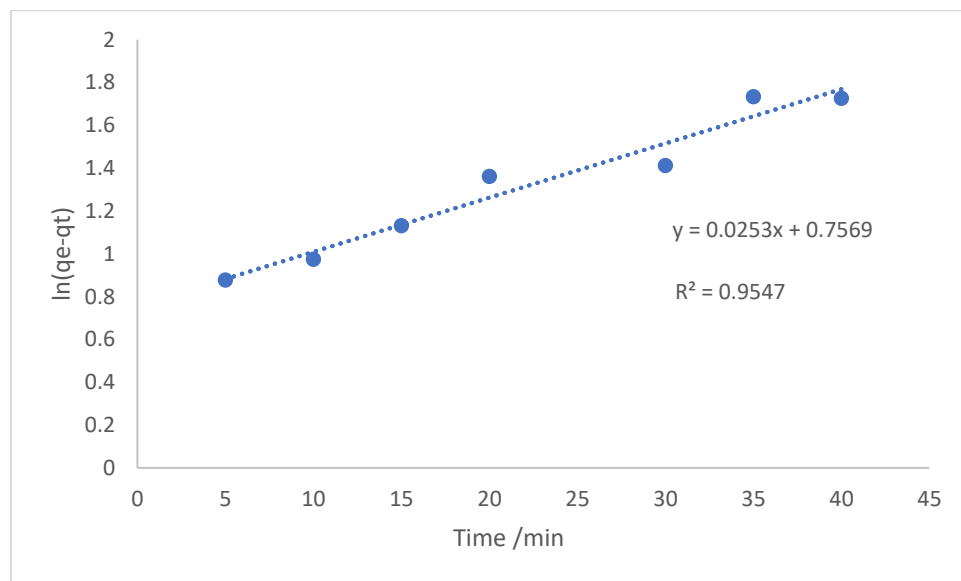


Figure 4.8 Pseudo first order kinetic model for the adsorption

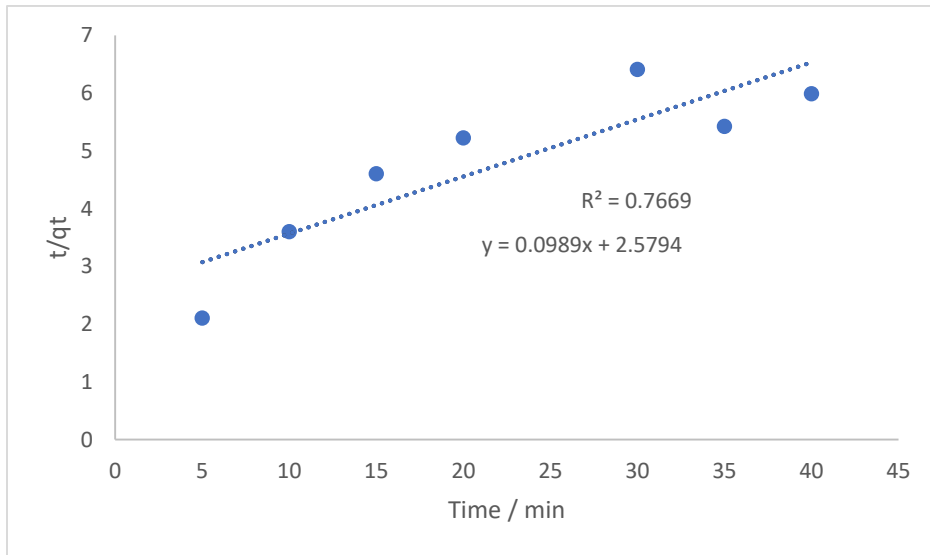


Figure 4.9 Pseudo second order kinetic model for the adsorption of CV

Table 4.2 The best fit experimental parameters to describe the adsorption

	Pseudo First order	Pseudo Second order
R ²	0.9547	0.7669
K1	-0.0582	
K2		39.6359

4.5 Adsorption thermodynamics model

The value of ΔG increases as the temperature of the process increases from 25 °C to 60 °C (**table 4.3**). This proves that the adsorption of CV onto CS biochar from water was a spontaneous process. At room temperature (25 °C) the Gibbs free energy has the most negative value ($\Delta G = -1468.70$ KJ/mol) and at 30 °C ($\Delta G = -350.78$ kJ/mol) these explains the spontaneity of the adsorption process which decreases with temperature. The value of K which is the dynamic equilibrium constant, is decreasing from 1.809 to 0.168 as temperature increase from 25°C to 60°C as shown in (**Table 4.3**). This reviews that the temperature affected the rate of attaining the equilibrium of the adsorption process under study. At low temperature the K value is large and ΔG is more negative is the evidence that removal of crystal violet dyes from water was spontaneous and attained equilibrium at a quicker rate than at higher temperatures (**Table 4.3**). The large value of correlation coefficient ($R^2 = 0.9039$) of the plot of the data obtained from this current study support the evidence that rate of reaching the equilibrium of the process under investigation was greatly affected by temperature (**Fig 4.11**)

Table 4.3 Thermodynamics parameters for the adsorption process

ΔG (Kj/mol)	K	$Temp$ (°C)
-1468.700227	1.809043408	25
-350.7780262	1.152094241	30
448.8087663	0.834311348	40
3193.121329	0.275598355	50
4421.305937	0.167875648	60

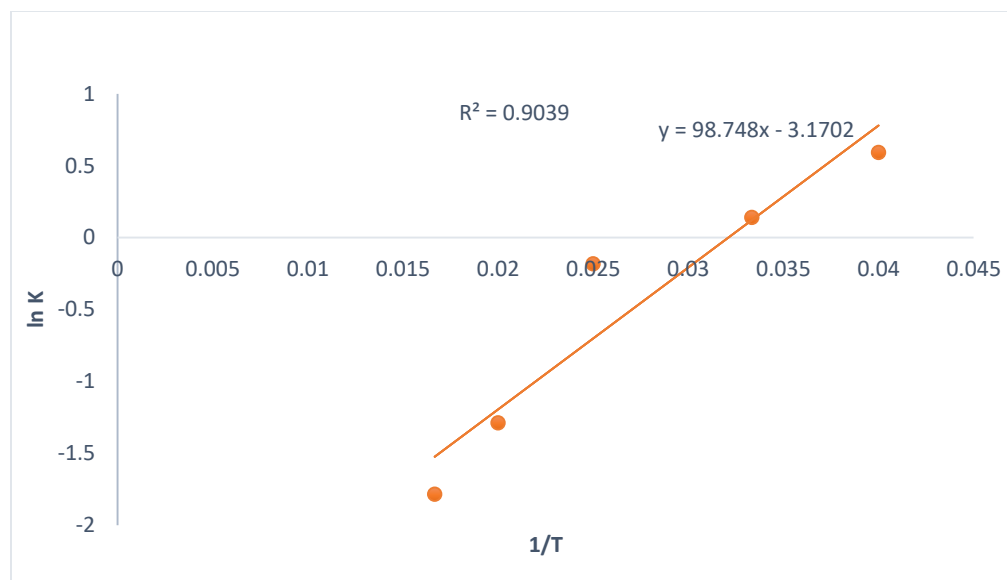


Figure 4.10 Thermodynamics plot of the adsorption process

The standard enthalpy changes of the reaction ($\Delta H = -0.821 \text{ kJ/mol}$) indicates that the adsorption process of pollutants was exothermic is supported by the negative values of H° for CV. The fact that the adsorbed amount decreases with increasing temperature already suggests that the adsorption process of pollutants was exothermic is supported by the negative values of H° for CV. This can be explained by the weakening of the adsorption forces caused by the rise in temperature between the adsorbed species and the carbon's active sites. The decrease in disorder at the solid-liquid interfaces is caused by the adsorption of CV a, as shown by the negative values of standard entropy, S° (Loulid., et al 2023) as shown in **Table 4.3**. The negative value of ΔS° (**Table 4.3**) shows that energy was utilized in the reaction hence less disorder of the system.

4.6 Comparisons of the findings of this work with the relevant literature

The pH affected the removal efficiency of the sorbent used in this study. As pH increased from 4 to 8 , the percentage removal of the contaminants increases from 46% to 62% respectively. This was to complement the results obtained in the literature which has the percentage removal of crystal violet from aqueous solution ranging from 72% to 84% at pH 2 to 8 respectively (Muhammad., et al 2019). Generally, the maximum removal efficiency of crystal violet from waste water by bio-sorbent(CS biochar) used in this work was 70.97%, which is close to the 80% removal efficiency obtained in the literature where unoptimized dead leaves of oak tree biochar was used to eliminate CV from aqueous solutions at pH 7, (Sulyman and Giarak, 2020) in **Table 2.1**

Chapter Five

5.0 Conclusion and Recommendation

The crystal violet (CV) dyes were successfully removed from water through adsorption onto porous surface of the corn stalks biochar. From the experiments carried out in this study, the following information about the adsorption process of CV were obtained;

- The standard enthalpy change, ($\Delta H = -0.821 \text{ kJ/mol}$) was negative which indicates exothermic process
- The Gibbs free energy (ΔG) was negative which become positive at elevated temperature above room temperature implying that the adsorption of CV spontaneous process and feasible at 25°C
- The standard entropy change ($\Delta S = -0.026 \text{ kJ/mol}^\circ\text{C}$) was negative meaning the system was less disorder, and the adsorption process was stable
- The adsorption followed pseudo first order reaction kinetics
- The adsorption study of CV onto corn stalk biochar was a monolayer adsorption (Langmuir adsorption isotherm modeling)
- The maximum percentage removal of crystal violet dyes from water was achieved at room temperature (70.97%)

The experimental data obtained in this study explains that low-cost corn stalks biochar can be used to treat water effluent containing dyes and mitigate the undesirable effects of dyes in the environment and water system. The future research should focus on the recovery of the biochar slug and the environmental impacts of the discharged corn stalk biochar, and also the chemical compounds and gases released when it is thrown into the environment and their toxicity.

6. References

- Almond, R.E., Grooten, M. and Peterson, T., 2020. *Living Planet Report 2020-Bending the curve of biodiversity loss*. World Wildlife Fund.
- Akhtar, N., Syakir Ishak, M.I., Bhawani, S.A. and Umar, K., 2021. Various natural and anthropogenic factors responsible for water quality degradation: A review. *Water*, 13(19), p.2660.
- Bullon, J., González Arrieta, M.A., Hernández Encinas, A. and Queiruga Dios, M.A., 2017. Manufacturing processes in the textile industry. *Expert Systems for fabrics production*.
- Seow, Y.X., Tan, Y.H., Mubarak, N.M., Kansedo, J., Khalid, M., Ibrahim, M.L. and Ghasemi, M., 2022. A review on biochar production from different biomass wastes by recent carbonization technologies and its sustainable applications. *Journal of Environmental Chemical Engineering*, 10(1), p.107017.
- Corcoran, E. ed., 2010. *Sick water?: the central role of wastewater management in sustainable development: a rapid response assessment*. UNEP/Earthprint.
- Carr, C. ed., 2012. *Chemistry of the textiles industry*. Springer Science & Business Media.
- Dai, Y., Zhang, N., Xing, C., Cui, Q. and Sun, Q., 2019. The adsorption, regeneration and engineering applications of biochar for removal organic pollutants: a review. *Chemosphere*, 223, pp.12-27.
- Alderete, B.L., da Silva, J., Godoi, R., da Silva, F.R., Taffarel, S.R., da Silva, L.P., Garcia, A.L.H., Júnior, H.M., de Amorim, H.L.N. and Picada, J.N., 2021. Evaluation of toxicity and mutagenicity of a synthetic effluent containing azo dye after advanced oxidation process treatment. *Chemosphere*, 263, p.128291.
- Chen, T., Zhang, Y., Wang, H., Lu, W., Zhou, Z., Zhang, Y. and Ren, L., 2014. Influence of pyrolysis temperature on characteristics and heavy metal adsorptive performance of biochar derived from municipal sewage sludge. *Bioresource technology*, 164, pp.47-54.
- Bhuiyan, M.R., Shaid, A., Bashar, M.M., Haque, P. and Hannan, M.A., 2013. A novel approach of dyeing jute fiber with reactive dye after treating with chitosan. *Open Journal of Organic Polymer Materials*, 2013.
- Mani, S. and Bharagava, R.N., 2018. Textile industry wastewater: environmental and health hazards and treatment approaches. In *Recent advances in environmental management* (pp. 47-69). CRC Press.
- Munagapati, V.S. and Kim, D.S., 2016. Adsorption of anionic azo dye Congo Red from aqueous solution by Cationic Modified Orange Peel Powder. *Journal of Molecular Liquids*, 220, pp.540-548.

Mani, S., Chowdhary, P., & Bharagava, R. N. 2019. Textile wastewater dyes: toxicity profile and treatment approaches. *Emerging and eco-friendly approaches for waste management*, 219-244.

Gürses, A., Açıkyıldız, M., Güneş, K., Gürses, M.S., Gürses, A., Açıkyıldız, M., Güneş, K. and Gürses, M.S., 2016. Classification of dye and pigments. *Dyes and pigments*, pp.31-45.

Al-Tohamy, R., Ali, S.S., Li, F., Okasha, K.M., Mahmoud, Y.A.G., Elsamahy, T., Jiao, H., Fu, Y. and Sun, J., 2022. A critical review on the treatment of dye-containing wastewater: Ecotoxicological and health concerns of textile dyes and possible remediation approaches for environmental safety. *Ecotoxicology and Environmental Safety*, 231, p.113160.

Kant, R., 2011. Textile dyeing industry an environmental hazard.

Al-Maliky, E.A., Gzar, H.A. and Al-Azawy, M.G., 2021, September. Determination of point of zero charge (PZC) of concrete particles adsorbents. In *IOP Conference Series: Materials Science and Engineering* (Vol. 1184, No. 1, p. 012004). IOP Publishing.

McBeath, A.V., Smernik, R.J., Krull, E.S. and Lehmann, J., 2014. The influence of feedstock and production temperature on biochar carbon chemistry: A solid-state ¹³C NMR study. *Biomass and Bioenergy*, 60, pp.121-129.

Gupta, M., Savla, N., Pandit, C., Pandit, S., Gupta, P.K., Pant, M., Khilari, S., Kumar, Y., Agarwal, D., Nair, R.R. and Thomas, D., 2022. Use of biomass-derived biochar in wastewater treatment and power production: A promising solution for a sustainable environment. *Science of the Total Environment*, p.153892.

Nejadshafiee, V. and Islami, M.R., 2019. Adsorption capacity of heavy metal ions using sultone-modified magnetic activated carbon as a bio-adsorbent. *Materials Science and Engineering: C*, 101, pp.42-52.

Huang, M., Li, Z., Luo, N., Yang, R., Wen, J., Huang, B., & Zeng, G. 2019. Application potential of biochar in environment: Insight from degradation of biochar-derived DOM and complexation of DOM with heavy metals. *Science of the Total Environment*, 646, 220-228.

Premarathna, K. S. D., Rajapaksha, A. U., Sarkar, B., Kwon, E. E., Bhatnagar, A., Ok, Y. S., & Vithanage, M. (2019). Biochar-based engineered composites for sorptive decontamination of water: A review. *Chemical Engineering Journal*, 372, 536-550.

- Dhruv Patel, D., & Bhatt, S. (2022). Environmental pollution, toxicity profile, and physico-chemical and biotechnological approaches for treatment of textile wastewater. *Biotechnology and Genetic Engineering Reviews*, 38(1), 33-86.
- Vikrant, K., Kim, K. H., Ok, Y. S., Tsang, D. C., Tsang, Y. F., Giri, B. S., & Singh, R. S. (2018). Engineered/designer biochar for the removal of phosphate in water and wastewater. *Science of the Total Environment*, 616, 1242-1260.
- Li, H., Dong, X., da Silva, E. B., de Oliveira, L. M., Chen, Y., & Ma, L. Q. (2017). Mechanisms of metal sorption by biochars: biochar characteristics and modifications. *Chemosphere*, 178, 466-478.
- Chaukura N, Murimba E.C, Gwenzi W. (2016b). Synthesis , characterisation and methyl orange adsorption capacity of ferric-oxide biochar nano-composites derived from pulp and paper sludge. *Applied Water Science* 1-12.
- Affat, S.S., 2021. Classifications, advantages, disadvantages, toxicity effects of natural and synthetic dyes: a review. *University of Thi-Qar Journal of Science*, 8(1), pp.130-135.
- Li, R., Zeng, K., Soria, J., Mazza, G., Gauthier, D., Rodriguez, R. and Flamant, G., 2016. Product distribution from solar pyrolysis of agricultural and forestry biomass residues. *Renewable Energy*, 89, pp.27-35.
- Samanta, A.K. and Konar, A., 2011. Dyeing of textiles with natural dyes. *Natural dyes*, 3(30-56).
- Zhang, W., Duo, H., Li, S., An, Y., Chen, Z., Liu, Z., ... & Wang, X. (2020). An overview of the recent advances in functionalization biomass adsorbents for toxic metals removal. *Colloid and Interface Science Communications*, 38, 100308.
- Pereira, L., & Alves, M. (2012). Dyes—environmental impact and remediation. *Environmental protection strategies for sustainable development*, 111-162.
- Singh, K., & Arora, S. (2011). Removal of synthetic textile dyes from wastewaters: a critical review on present treatment technologies. *Critical reviews in environmental science and technology*, 41(9), 807-878.

- Wong, J. K. H., Tan, H. K., Lau, S. Y., Yap, P. S., & Danquah, M. K. (2019). Potential and challenges of enzyme incorporated nanotechnology in dye wastewater treatment: A review. *Journal of environmental chemical engineering*, 7(4), 103261.
- Muhammad, U. L., Zango, Z. U., & Kadir, H. A. 2019. Crystal violet removal from aqueous solution using corn stalk biosorbent. *Science World Journal*, 14(1), 133-138.
- Laurichesse, S., & Avérous, L. (2014). Chemical modification of lignins: Towards biobased polymers. *Progress in polymer science*, 39(7), 1266-1290.
- Zbair, M., Ainassaari, K., Drif, A., Ojala, S., Bottlinger, M., Pirilä, M., ... & Brahmi, R. 2018. Toward new benchmark adsorbents: preparation and characterization of activated carbon from argan nut shell for bisphenol A removal. *Environmental Science and Pollution Research*, 25, 1869-1882.
- Singh, S., Anil, A. G., Khasnabis, S., Kumar, V., Nath, B., Adiga, V., ... & Ramamurthy, P. C. 2022. Sustainable removal of Cr (VI) using graphene oxide-zinc oxide nanohybrid: Adsorption kinetics, isotherms and thermodynamics. *Environmental Research*, 203, 111891.
- Peiris, C., Nayanathara, O., Navarathna, C. M., Jayawardhana, Y., Nawalage, S., Burk, G., ... & Gunatilake, S. R. (2019). The influence of three acid modifications on the physicochemical characteristics of tea-waste biochar pyrolyzed at different temperatures: a comparative study. *RSC advances*, 9(31), 17612-17622.
- Chen, X., Ma, R., Luo, J., Huang, W., Fang, L., Sun, S. and Lin, J., 2021. Co-microwave pyrolysis of electroplating sludge and municipal sewage sludge to synergistically improve the immobilization of high-concentration heavy metals and an analysis of the mechanism. *Journal of Hazardous Materials*, 417, p.126099.
- Loulidi, I., Jabri, M., Amar, A., Kali, A., A. Alrashdi, A., Hadey, C., ... & Boukhlifi, F. (2023). Comparative Study on Adsorption of Crystal Violet and Chromium (VI) by Activated Carbon Derived from Spent Coffee Grounds. *Applied Sciences*, 13(2), 985.
- Chakraborty, S., Chowdhury, S., & Saha, P. D. (2011). Adsorption of crystal violet from aqueous solution onto NaOH-modified rice husk. *Carbohydrate Polymers*, 86(4), 1533-1541.

Misra, M., Akansha, K., Sachan, A., & Sachan, S. G. 2020. Removal of dyes from industrial effluents by application of combined biological and physicochemical treatment approaches. *Combined application of physico-chemical & microbiological processes for industrial effluent treatment plant*, 365-407.

Muhammad, U.L., Zango, Z.U. and Kadir, H.A., 2019. Crystal violet removal from aqueous solution using corn stalk biosorbent. *Science World Journal*, 14(1), pp.133-138

Appendix

i. Raw data and spectroscopic data





The calibration curve for cryastal violet dyes obtained



Raw data

Time (min)	qt (mg/g)	Co (mg/L)	Ce (mg/L)	ln (Co/Ce)	qe (mg/g)	Ct (mg/L)
5	2.37	125	89.06	0.2914223	2.6955	93.4
10	2.775	125	85	0.3509769	3	88
15	3.255	125	78	0.4264844	3.525	81.6
20	3.825	125	66	0.5242486	4.425	74
30	4.68	125	61	0.6915484	4.8	62.6
35	6.45	125	34	1.1647520	6.825	39
40	6.675	125	33.43	1.2447947	6.86775	36

Table 4: experimental data 1

Pseudo 1st order

pseudo 2nd order

ln(qe-qt)	t/qt	slope=- k1/2.303	K1	K2=1/intercept*qe2	slope=1/qe	qe=1/slope
0.87716629	2.109	0.0253	-0.05826	39.63589975		10.111223
0.97419092	3.603					
1.13092313	4.608					
1.36116919	5.228					
1.41304620	6.410					
1.73346769	5.426					
1.72685736	5.992					

Table 5 ; experimental data 2

Freundlich isotherm data

Ce (mg/L)	qe (mg/g)	ln Ce	ln qe	Slope = n	Intercep t = ln K	K	Co (mg/L)	Mass, m / mg
19.31	0.03225	2.96062309 6	- 3.43423723 6	-1.2239			23.61	10
15.63	0.05985	2.74919214 4	- 2.81591384 7				23.61	10
15	0.06457 5	2.70805020 1	- 2.73992794				23.61	10
7.39	0.12165	2.00012773 5	- 2.10660721				23.61	10

Table 6; experimental data 3

qe (mg/g)	Ce/qe	Slope = 1/Qo	intercept= 1/Qo*K	Qo (mg/g)	K
860	0.022453488	0.0012	0.0019	833.3333333	1.583333333
798	0.019586466	0.0012	0.0019	833.3333333	1.583333333
574	0.026132404	0.0012	0.0019	833.3333333	1.583333333
811	0.009112207	0.0012	0.0019	833.3333333	1.583333333

Table 7 ; Langmuir adsorption isotherm experimental data 1

Co (mg/L)	Volume, V / L	Mass, m / mg	log Ce	log qe	ql = 1/(1+Kco)
23.61	0.075	0.5	1.285782274	2.934498451	0.02605354
23.61	0.075	1	1.193958978	2.902002891	0.02605354
23.61	0.075	1.5	1.176091259	2.758911892	0.02605354
23.61	0.075	2	0.868644438	2.909020854	0.02605354

Table 8; Langmuir adsorption isotherm experimental data 2

Thermodynamics experimental data

$q_e(\text{mg/g})$	$C_o(\text{mg/L})$	$\ln(q_e/C_e)$	G	K	$\text{Temp}/^\circ\text{C}$	$1/T$	$\text{Slope} = -\Delta H/R$	$\text{Intercept} = \Delta S/R$	$\Delta H(\text{kJ/mol})$	$\Delta S(\text{kJ/mol})$
9.0018	125	0.5927 98202	- 1468.7002 27	1.809 0434 08	25	0.04	98.748	-3.1702	- 0.820 99087 2	- 0.0263 57043
8.802	125	0.1415 81365	- 350.77802 62	1.152 0942 41	30	0.0333 33333				
8.6017 5	125	- 0.1811 48627	448.80876 63	0.834 3113 48	40	0.025				
7.3695	125	- 1.2888 1071	3193.1213 29	0.275 5983 55	50	0.02				
6.48	125	- 1.7845 31766	4421.3059 37	0.167 8756 48	60	0.0166 66667				

Table 9

The effect of temperature

$C_o(\text{mg/L})$	$C_t(\text{mg/L})$	%R	V/ml	mass, m/g	$q_t(\text{mg/L})$	Time/ mins	%R	pH
125	34.04	72.768				10	14.43	10
34.04	28.77	15.48178 613				20	34.05	15
28.77	22.09	23.21863 052				30	68.05	20
22.09	21	4.934359 439				40	70.97	25
		0						

Table 10; experimental data of the effect of temperature

The effect of pH

initial pH	final pH	Δ pH	pH
2	3.9	-1.9	2
4	4.8	-0.8	4
6	6.4	-0.4	6
8	7.8	0.2	8

Table 11; experimental data